

## Thermoelectric properties of polycrystalline tetragonal $\text{SrCu}_2\text{O}_2$

Octolia Togibasa Tambunan<sup>a</sup>, Jaeyeong Kim<sup>a</sup>, Il-Ho Kim<sup>b</sup>, Chang Uk Jung<sup>a</sup>, Bo Wha Lee<sup>a</sup> and Chunli Liu<sup>a,\*</sup>

<sup>a</sup>Department of Physics, Hankuk University of Foreign Studies, Yongin, 449-791, Korea

<sup>b</sup>Department of Material Science and Engineering, Chungju National University, Chungju, Chungbuk, 380-702, Korea

In this study, we report the successful fabrication of polycrystalline tetragonal  $\text{SrCu}_2\text{O}_2$  by a solid state reaction and the dependence of its thermoelectric properties on the sintering temperature. Two sintering temperatures, 1093 K and 1143 K, were used in the solid state reaction process. A *p*-type semiconducting behavior was observed for both samples. In the temperature range of 423 to 923 K, the  $\text{SrCu}_2\text{O}_2$  sintered at 1093 K shows a relatively higher conductivity, power factor, and figure of merit as compared to the  $\text{SrCu}_2\text{O}_2$  sintered at 1143 K. At 923 K, the Seebeck coefficient and the power factor for the  $\text{SrCu}_2\text{O}_2$  sintered at 1093 K are 298 mV/K and  $2 \times 10^{-6}$  W/mK<sup>2</sup>, respectively. These values are comparable to the thermoelectric performance of polycrystalline *p*-type  $\text{CuAlO}_2$ , suggesting that polycrystalline  $\text{SrCu}_2\text{O}_2$  prepared with optimized conditions could be used for thermoelectric applications.

**Key words:**  $\text{SrCu}_2\text{O}_2$ , Solid-state reaction, Polycrystalline, Thermoelectric property, Temperature effect.

### Introduction

Thermoelectric materials can convert thermal energy directly to electrical energy via the Seebeck effect induced by a temperature difference in solid materials, so they are widely used for energy conversion between electricity and heat. The thermoelectric performance is evaluated by the figure of merit,  $Z = \alpha^2 \sigma / \kappa$  [1] where  $\alpha$  is the Seebeck coefficient,  $\sigma$  is the electrical conductivity, and  $\kappa$  is the thermal conductivity of the material. Although oxidation resistant at high temperature, conventional oxide materials are usually not suitable for use as thermoelectric materials due to their low electrical conductivity. On the other hand, conducting oxides, such as  $\text{Na}_x\text{CoO}_2$ ,  $(\text{Zn}_{1-x}\text{Al}_x)\text{O}$ , and  $\text{CaMnO}_3$  [2-4] have recently attracted research attention for their possible thermoelectric application over a wide temperature range. The discovery of *p*-type conducting oxides, such as  $\text{CuAlO}_2$  and  $\text{SrCu}_2\text{O}_2$  [5, 6], provided promising candidates not only for full oxide electronic devices but also for thermoelectric applications. The studies on both bulk and thin film  $\text{CuAlO}_2$  showed that relatively good thermoelectric properties can be achieved through careful optimization of the preparation process [5, 7].

Similar to  $\text{CuAlO}_2$ ,  $\text{SrCu}_2\text{O}_2$  (SCO) is another promising *p*-type transparent conducting oxide, but  $\text{SrCu}_2\text{O}_2$  thin films can be deposited with pulsed laser deposition at a lower temperature than  $\text{CuAlO}_2$  [8, 9].  $\text{SrCu}_2\text{O}_2$  has a tetragonal crystal structure with bulk lattice constants of  $a = 5.48 \text{ \AA}$  and  $c = 9.82 \text{ \AA}$ . In the  $\text{SrCu}_2\text{O}_2$  crystal lattice, Sr atoms are at the center of a dumbbell O-Cu-O unit,

and the O-Cu-O dumbbells are connected to form one-dimensional zig-zag chains along [100] and [010] directions [10]. The origin of *p*-type behavior appears to reside in the +1 valence of the Cu cation. Band structure calculations for  $\text{SrCu}_2\text{O}_2$  indicate that it is a direct band gap material with a band edge at the zone center. The reported experimental band gap value of  $\text{SrCu}_2\text{O}_2$  is about 3.3 eV [6]. So far detailed studies on the thermoelectric properties of  $\text{SrCu}_2\text{O}_2$  have been rare. Additionally, the fabrication of polycrystalline  $\text{SrCu}_2\text{O}_2$  is not trivial due to the difficulty in controlling the valence state of Cu ions. In this study, we report the successful preparation of polycrystalline  $\text{SrCu}_2\text{O}_2$  using a conventional solid state reaction method and the effect of the sintering temperature on the thermoelectric properties of  $\text{SrCu}_2\text{O}_2$ . Our results show that the sintering temperature alone could affect the microstructure of the material, and thus affect its thermoelectric properties.

### Experimental

$\text{SrCu}_2\text{O}_2$  ceramics have been reported to be synthesized mainly using a solid state reaction [6, 11, 12]. The essential point of  $\text{SrCu}_2\text{O}_2$  synthesis is to reduce the strong localization of oxygen ions to the positive holes on the valence band edge, which originates from the large electronegativity of oxygen. In this study  $\text{SrCu}_2\text{O}_2$  ceramics were synthesized by sintering a stoichiometric mixture of  $\text{CuO}$  (99.5%) and  $\text{SrCO}_3$  (99.999%) powders with a Cu/Sr atomic ratio of 2 : 1. The mixed powder was first ground for 1 h, and then calcined at 1073 K in a flowing  $\text{N}_2$  ambient. Several calcination recipes were tested in terms of temperature and reactive atmosphere. The optimized process with respect to the final phase of the ceramic pellet is a two-step process. First, the mixed powder

\*Corresponding author:

Tel : +82-31-3304733

Fax: +82-31-3304566

E-mail: chunliliu@hufs.ac.kr

was rapidly heated to 1073 K at 20 K/min in an alumina boat and calcined for 5 h, then reground. In the second step, the powder was slowly heated to 1073 K at 5 K/min and calcined for 10 h, then reground. The slow heating and regrinding processes were repeated for 3 times, i.e., heating for a total of 30 h. The final product was pressed into pellets by hydrostatic pressure of approximately 113 MPa. These grey compact pellets were sintered at either 1093 K or 1143 K for 10 h in N<sub>2</sub> gas.

The crystalline structure of the sintered samples was analyzed by X-ray diffraction (XRD; Rigaku Miniflex Diffractometer) using Cu-K $\alpha$  radiation. The microstructure of the samples was investigated with field emission scanning electron microscope (FE-SEM; Hitachi S-4300). The electrical conductivity and the Seebeck coefficient were measured using an Ulvac-Riko ZEM2-M8 system, and the thermal conductivity was measured using an Ulvac-Riko TC7000 system. The thermoelectric measurements were carried out from 423 to 923 K.

## Result and Discussion

### Structural properties

The phase evolution of the ceramic during calcination and sintering is shown through the XRD patterns in Fig. 1. Only peaks from SrCuO<sub>2</sub> and CuO are observed after the rapid heating step [Fig. 1(a)]. During the slow heating process, the peak intensity of CuO and SrCuO<sub>2</sub> is reduced rapidly with increasing heating time, whereas the peaks from SrCu<sub>2</sub>O<sub>2</sub> increase and become dominant. After 3 slow heating cycles, peaks from SrCuO<sub>2</sub> and CuO almost completely disappeared [Fig. 1(b)-(c)]. Risold *et al.* [13] noted that the invariant equilibria in the Sr-Cu-O system for SrCu<sub>2</sub>O<sub>2</sub> (1284 K) is higher than for SrCuO<sub>2</sub> (1192 K). We also found that there were mixed phase of SrCuO<sub>2</sub> and SrCu<sub>2</sub>O<sub>2</sub> in the sintered pellet if no

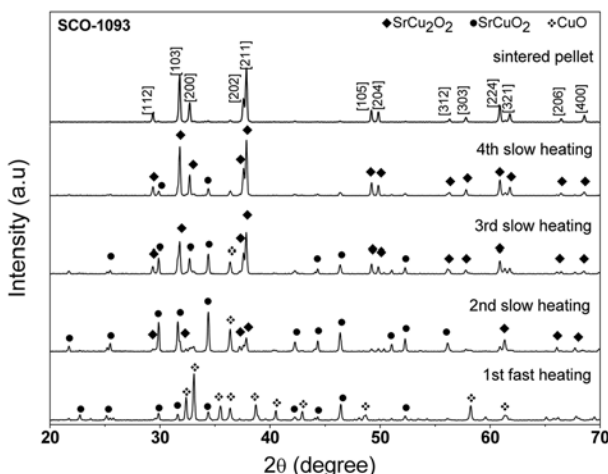


**Fig. 1.** XRD patterns showing the phase evolution during fabrication of the SrCu<sub>2</sub>O<sub>2</sub> ceramics after (a) fast heating, (b) 1<sup>st</sup> slow heating, (c) 2<sup>nd</sup> slow heating, (d) 3<sup>rd</sup> slow heating, and (e) sintering. The symbols  $\blacklozenge$ ,  $\bullet$ , and  $\divideontimes$  represent peaks of SrCu<sub>2</sub>O<sub>2</sub>, SrCuO<sub>2</sub>, and CuO, respectively.

rapid heating process was applied. Therefore we propose that the effect of the rapid heating step is to limit the formation of SrCuO<sub>2</sub> at a lower temperature.

The calcined powder was then pressed into a pellet and sintered at a higher temperature of 1093 K or 1143 K to get a single-phased polycrystalline SrCu<sub>2</sub>O<sub>2</sub> ceramic, which will be referred as SCO-1093 and SCO-1143 hereafter. Ceramics sintered at both temperatures show the same peaks in the XRD patterns as shown in Fig. 1(e). All of these peaks are identified to originate from SrCu<sub>2</sub>O<sub>2</sub> with a tetragonal crystalline structure [12].

The effect of different sintering temperatures on the microstructure of the SrCu<sub>2</sub>O<sub>2</sub> ceramic has been investigated. The bulk densities of the SrCu<sub>2</sub>O<sub>2</sub> ceramic sintered at 1093 K and 1143 K are 4.230 g/cm<sup>3</sup> and 4.510 g/cm<sup>3</sup>, respectively, indicating a higher density at a higher sintering temperature. In consistent with this is that SCO-1093 looks more porous than SCO-1143 from the FE-SEM surface morphology images shown in Fig. 2.

### Thermoelectric properties

Fig. 3 shows the temperature dependence of the electrical conductivity ( $\sigma$ ) of SrCu<sub>2</sub>O<sub>2</sub>. For both samples, the electrical conductivity increases with temperature at first, then decreases slightly near 923 K. The change of the electrical conductivity with temperature indicates a semiconducting behavior. However, the overall conductivity is quite low,

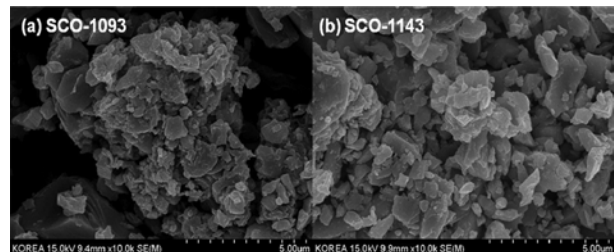


**Fig. 2.** The FE-SEM images of the surface of SrCu<sub>2</sub>O<sub>2</sub> sintered at (a) 1093 K and (b) 1143 K.

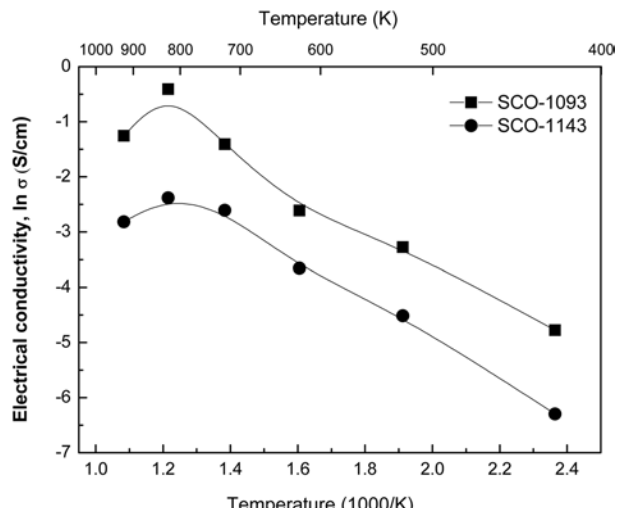


**Fig. 3.** Temperature dependence of the electrical conductivity of SrCu<sub>2</sub>O<sub>2</sub> sintered at (■) 1093 K and (●) 1143 K.

with highest values of 0.67 and 0.09 S/cm for SCO-1093 and SCO-1143, respectively. The temperature dependence of  $\sigma$  follows the Arrhenius law  $\sigma = \sigma_0 \exp(\Delta E_a/kT)$ , where  $\sigma_0$  is the pre-exponential factor,  $\Delta E_a$  is the activation energy of the electrical conduction,  $k$  is the Boltzmann constant, and  $T$  is the absolute temperature. From the slope of the  $\ln\sigma \sim 1/T$  curve, the activation energy has been calculated to be  $\sim 0.26$  eV. This value is similar to the value reported for a  $\text{SrCu}_2\text{O}_2$  thin film (0.2 eV) [6].

In order to identify the major conduction type of  $\text{SrCu}_2\text{O}_2$ , measurements of the Seebeck coefficients ( $\alpha$ ) have been carried out. As shown in Fig. 4, the Seebeck coefficients are positive for all measured temperatures, indicating *p*-type conductivity [6]. The Seebeck coefficient values for both samples decrease up to 723 K and then show an increase. The Seebeck coefficient is affected by the carrier concentration ( $n_c$ ) in the following way :  $\alpha \approx r \cdot \ln n_c$  [5], where  $r$  is a scattering factor. An increase in the carrier concentration can cause a decrease in the Seebeck coefficient. Therefore, the temperature dependence of the Seebeck coefficient is roughly consistent with the electrical conductivity properties shown in Fig. 3. It is noted that although the electrical conductivity of SCO-1093 is higher, the Seebeck coefficient of SCO-1093 has lower values than that of SCO-1143. Additional to the carrier concentration, the electrical conductivity is also strongly affected by the mobility of the carriers, and both factors are strongly affected by the microstructure of SCO. The two SCO ceramics should have different microstructural properties due to the variation of the sintering temperature as indicated by the surface morphology shown in Fig. 2 and their densities, which could result in the observed diversity of the electrical conductivities and Seebeck coefficients.

The power factor ( $\alpha^2\sigma$ ) shown in Fig. 5 represents the electrical contribution to the thermoelectric performance. The power factor increases with temperature for both samples, with SCO-1093 showing a slightly higher average value over the measured temperature range. At 923 K, the power factor values are about  $2 \times 10^{-6}$  W/mK<sup>2</sup> for both samples. Although the SCO ceramics show similar

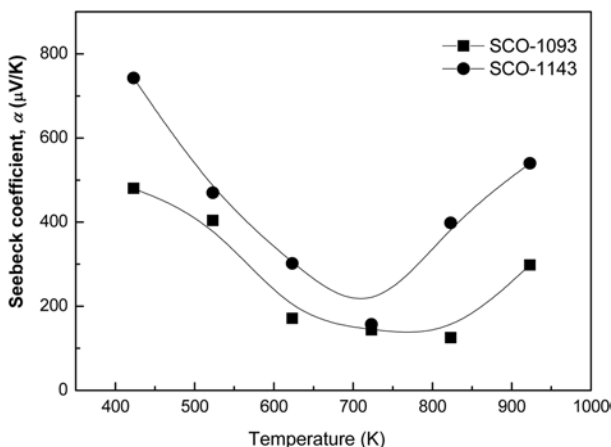


Fig. 4. Seebeck coefficient as a function of temperature for  $\text{SrCu}_2\text{O}_2$  sintered at (■) 1093 K and (●) 1143 K.

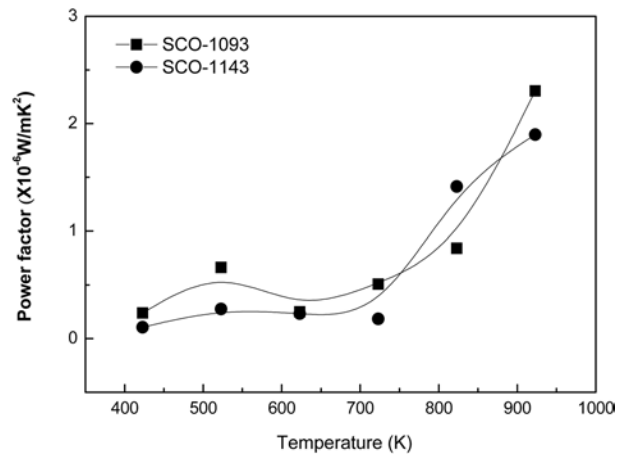


Fig. 5. Power factor as a function of temperature for  $\text{SrCu}_2\text{O}_2$  sintered at (■) 1093 K and (●) 1143 K.

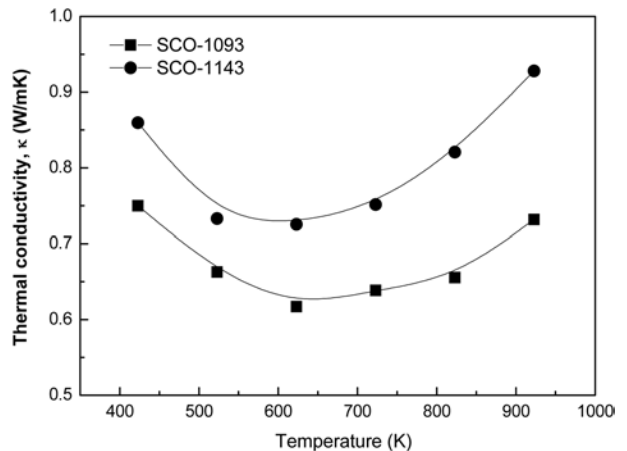
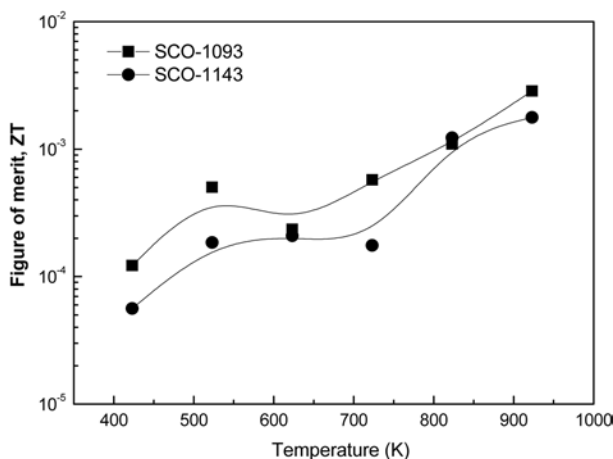


Fig. 6. Temperature dependence of the thermal conductivity of  $\text{SrCu}_2\text{O}_2$  sintered at (■) 1093 K and (●) 1143 K.

Seebeck coefficients with the reported value for polycrystalline  $\text{CuAlO}_2$ , the power factor of SCO is about one order lower than  $\text{CuAlO}_2$  [5], which is mainly due to the low electrical conductivity. It has been reported that for a *p*-type oxide doping can effectively improve the power factor through an increased carrier concentration [3, 6, 14-15], so we expect that the thermoelectric properties of the  $\text{SrCu}_2\text{O}_2$  ceramics could also be enhanced through doping. A related study will be carried out in our future work.

Fig. 6 shows the variation of the thermal conductivity ( $\kappa$ ) with temperature. The thermal conductivity decreases first then increases as the measurement temperature goes higher. The value of  $\kappa$  of SCO-1093 varies from 0.61 to 0.74  $\text{W/mK}$ , whereas that of SCO-1143 ranges from 0.73 to 0.93  $\text{W/mK}$ . These values are about 10% of those reported for other oxide thermoelectric materials such as  $\text{TiO}$  [16] and  $\text{CaMnO}_3$  [4]. From the definition of figure of merit, i.e.  $Z = \alpha^2\sigma/\kappa$ , it is clear that a low value of  $\kappa$  is necessary to achieve a high value of  $Z$ . The relatively low  $\kappa$  value of SCO ceramics could be attributed to a high mean atomic mass and strong phonon scattering, which implies an advantage of SCO as a potential



**Fig. 7.** Dimensionless figure of merit as a function of temperature for  $\text{SrCu}_2\text{O}_2$  sintered at (■) 1093 K and (●) 1143 K.

thermoelectric material [17, 18].

The dimensionless figure of merit  $ZT$  is plotted in Fig. 7 as a function of temperature. Similar to the power factor, the value of  $ZT$  increases with the measurement temperature, and reaches up to  $2.86 \times 10^{-3}$  and  $1.78 \times 10^{-3}$  at 923 K for SCO-1093 and SCO-1143, respectively. These values are somewhat lower than the ideal  $ZT$  value of 1 for a perfect thermoelectric material. The relatively low  $ZT$  of the SCO ceramics is mainly due to the low electrical conductivity. Since incorporating appropriate dopants, such as potassium or calcium, can effectively increase the carrier concentration of  $\text{SrCu}_2\text{O}_2$  [6, 15], the figure of merit could also be improved by doping.

## Conclusion

Single-phase tetragonal  $\text{SrCu}_2\text{O}_2$  ceramic pellets were successfully prepared through solid-state reaction and the effect of the sintering temperature on the thermoelectric properties was investigated. A *p*-type conductive behavior is confirmed from positive Seebeck coefficients over all the measured temperature. In the temperature range of 423 to 923 K, the thermoelectric properties of SCO-1093 are better than those of SCO-1143, judging from the power factor and the dimensionless figure of merit,  $ZT$ . The Seebeck coefficient of the polycrystalline  $\text{SrCu}_2\text{O}_2$  is comparable to the reported results of *p*-type  $\text{CuAlO}_2$ , but doping appears to be necessary in order to improve the electrical conductivity and thermoelectric properties for practical applications.

## Acknowledgments

This study was supported by the Basic Science Research Programs (20090088632 and 20090074218) and the Mid-career Research Program (20090084750) through the National Research Foundation of Korea (NRF) grant funded by the Korea government (MEST); the Fundamental R&D Program for Core Technology of Materials and the Regional Innovation Center (RIC) Program grant funded by the Ministry of Knowledge Economy, Republic of Korea.

## References

1. H.J. Goldsmid, in "CRC Handbook of Thermoelectrics: Conversion Energy and Figure of Merit", edited by D. M. Rowe, CRC Press LLC, Boca Raton (1995).
2. D.J. Singh and D. Kasinathan, *J. Electron. Mater.* 36 (2007) 736-739.
3. T. Tsubota, M. Ohtaki, K. Eguchi and H. Arai, *J. Mater. Chem.* 7 (1997) 85-90.
4. J.W. Park, D.H. Kwak, S.H. Yoon and S.C. Choi, *J. Alloys and Comp.* 487 (2009) 550-555.
5. K. Park, K.Y. Ko and W.S. Seo, *J. Eur. Ceram. Soc.* 25 (2005) 2219-2222.
6. A. Kudo, H. Yanagi, H. Hosono and H. Kawazoe, *Appl. Phys. Lett.* 73 (1998) 220-222.
7. A.N. Banerjee, R. Maity, P.K. Ghosh and K.K. Chattopadhyay, *Thin Solid Films*, 474 (2005) 261-266.
8. E.L. Papadopoulou, Z.A. Viskadourakis, A.V. Pennos, G. Huyberechts and E. Aperathitis, *Thin Solid Films*, 516 (2008) 1449-1452.
9. H. Kawazoe, M. Yasukawa, H. Hyodo, M. Kurita, H. Yanagi and H. Hosono, *Nature*, 389 (1997) 939-942.
10. V. Varadarajan, D.P. Norton and J.D. Budai, *Thin Solid Films*, 488 (2005) 173-177.
11. C.C.B. Lynch, R.G. Egglett and D.S.L. Law, *Chem. Phys. Lett.* 401 (2005) 223-226.
12. E. Bobeico, F. Varsano, C. Minarini and F. Roca, *Thin Solid Films*, 444 (2003) 70-74.
13. D. Risold, B. Hallstedt and L.J. Gauckler, *J. Am. Ceram. Soc.* 80 (1997) 527-536.
14. K. Park, K.Y. Ko, H.C. Kwon and S. Nahm, *J. Alloys and Comp.* 437 (2007) 1-6.
15. S. Sheng, G. Fang, C. Li, Z. Chen, S. Ma, L. Fang and X. Zhao, *Semicond. Sci. Technol.* 21 (2006) 586-590.
16. N. Okinaka and T. Akiyama, in Proceedings of the 24<sup>th</sup> International Conference on Thermoelectrics, (IEEE 2005) p.34.
17. Q. He, Q. Hao, G. Chen, B. Poudel, X. Wang, D. Wang and Z. Ren, *Appl. Phys. Lett.* 91 (2007) 052505.
18. M.R. Winter and D.R. Clarke, *J. Am. Ceram. Soc.* 90 (2007) 533-540.